Barker, P.F., Camerlenghi, A., Acton, G.D., and Ramsay, A.T.S. (Eds.)
Proceedings of the Ocean Drilling Program, Scientific Results Volume 178

31. Magnetic Polarity Stratigraphy from Downhole Logs, West Antarctic Peninsula, ODP Leg 178[1]

Trevor Williams,[2] Veronique Louvel,[3] and C. Lauer-Leredde[4]

ABSTRACT

Magnetic field strength and magnetic susceptibility were logged with the geological high-resolution magnetic tool (GHMT) at three of the holes drilled during Ocean Drilling Program Leg 178 to the west of the Antarctic Peninsula. Polarity stratigraphies derived from the GHMT logs bear close resemblance to the polarities determined from core paleomagnetism at two of the holes and were used for magnetostratigraphic dating, especially in intervals where no core was recovered.

Polarity is determined in the following way. First, the susceptibility log is used to determine the induced magnetization of the sediment. Then the background field, the field of the metal drill pipe, and the field anomaly of the sediment's induced magnetization are removed from the measured total field to leave the downhole anomaly of the sediment's remanent magnetization. The sign (positive or negative) of this anomaly gave a good polarity stratigraphy for Holes 1095B and 1096C, which are located in sediment drifts. A further step, correlation analysis, is based on the fact that in an interval of normal polarity sediment the remanent anomaly will correlate with the induced anomaly, whereas in reversed polarity sediment they will anticorrelate.

The magnetite-rich, fine-grained sediments found in the two holes drilled into the sediment drift have a ratio of remanent to induced magnetization (the Koenigsberger ratio) of ~1. In contrast, the coarser-grained diamict sediments on the shelf have a Koenigsberger ratio of ~0.2, and extracting the remanent part of the downhole anomaly is much more difficult.

[1] Williams, T., Louvel, V., and Lauer-Leredde, C., 2002. Magnetic polarity stratigraphy from downhole logs, West Antarctic Peninsula, ODP Leg 178. *In* Barker, P.F., Camerlenghi, A., Acton, G.D., and Ramsay, A.T.S. (Eds.), *Proc. ODP, Sci. Results,* 178, 1–23 [Online]. Available from World Wide Web: <http://www-odp.tamu.edu/publications/178_SR/VOLUME/CHAPTERS/SR178_31.PDF>. [Cited YYYY-MM-DD]
[2] Lamont-Doherty Earth Observatory–Borehole Research Group, Route 9W, Palisades NY 10964, USA. **trevor@ldeo.columbia.edu**
[3] Laboratoire de Mesures en Forage, ODP-NEB, BP 72, 13545 Aix-en-Provence Cedex 4, France.
[4] ISTEEM, Université Montpellier 2, Place Eugene Bataillon, 34095 Montpellier Cedex 5, France.

Initial receipt: 3 October 2000
Acceptance: 12 December 2001
Web publication: 25 April 2002
Ms 178SR-222

By the comparison of core and log results, we can assess the viability of the GHMT polarities in detail, what proportion of the overprint in the cores is imparted by the coring process, and whether any paleointensity information is extractable from the GHMT logs.

INTRODUCTION

During Ocean Drilling Program (ODP) Leg 178, nine sites were drilled off the western coast of the Antarctic Peninsula with the aim of deducing the history of the peninsula's ice sheet over the last 10 m.y. (Fig. F1) (Barker, Camerlenghi, Acton, et al., 1999). Three sites were drilled into sediment drifts on the continental rise to provide a continuous but distal record of glacier output. This record is also influenced by the ocean current system. Two successful sites were drilled into the shelf to provide a proximal but discontinuous and poorly dated record of glacial activity. Two of the rise sites (Sites 1095 and 1096) and one of the shelf sites (Site 1103) were logged with downhole logging tools.

The geological high-resolution magnetic tool (GHMT) (Roperch et al., 1993) was deployed at all three of the logged sites. It comprises two sondes, the susceptibility measurement sonde (SUMS) and the nuclear resonance magnetometer sonde (NMRS). The SUMS measures the magnetic susceptibility in the formation surrounding the borehole. The susceptibility measurement is primarily dependent on the concentration of ferrimagnetic minerals (particularly magnetite) in the formation. In this environment, it can be interpreted in terms of magnetite input from terrestrial sources and magnetite dissolution. The NMRS measures the total magnetic field in the borehole using a proton-precession magnetometer (it does not measure the direction of the field). The major contribution to the magnetic field measurement is the field generated in the Earth's core, with lesser contributions from local seafloor anomalies, the drill string, and the remanent and induced magnetization of the sediment surrounding the borehole. The time-dependant magnetic field of the magnetosphere also contributes. We determine the polarity of the remanent magnetization by two methods: (1) taking the sign of the remanent anomaly (a positive anomaly corresponds to normal polarity and a negative anomaly corresponds to reversed polarity) and (2) the correlation analysis method (Vibert-Charbonnel, 1996), based on the fact that in an interval of normal polarity sediment the remanent anomaly will correlate with the induced anomaly, whereas in reversed polarity sediment they will anticorrelate.

The GHMT data from Leg 178 and the other ten ODP legs during which the GHMT was run are available at: **http://www.ldeo.columbia.edu/BRG/ODP/DATABASE**.

LOG DATA REPEATABILITY

There is generally good repeatability in both absolute value and shape of the susceptibility and the magnetic field logs, indicating that the logs are of good quality (Fig. F2). However, there are some differences in the details between the two passes, such as the presence of spikes (discussed below) and different depth positioning of some features, which we ascribe mainly to the high ship heave during logging.

The magnetic field logs for Holes 1095B and 1103A contain brief jumps in the field values (spikes). The magnetic field logs from Hole

F1. Bathymetric map of the West Antarctic Peninsula area, Leg 178, p. 12.

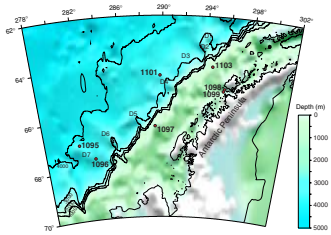

F2. Comparison of the two passes of the GHMT tool, Holes 1095B and 1096C, p. 13.

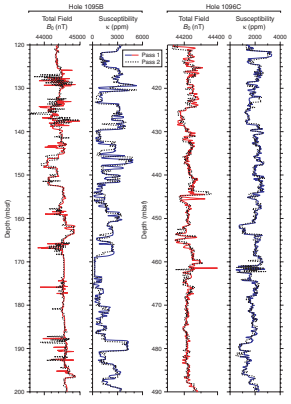

1096C contain far fewer spikes. There are likely two origins for the spikes because some spikes repeat at the same depth in successive logging runs (implying an origin in the formation), but others do not (implying a transient problem with the tool). It is known that spikes can occur when the tool is struck sharply (this was found during Leg 188 to be caused by a loose fitting inside the tool), and this could certainly happen downhole if the tool hit the borehole wall. Most of the spikes are accompanied by a drop in the tool voltage at the same depth. We have used this observation to clean spikes from the Hole 1095B magnetic field log used in the polarity analyses. Values at depths where the voltage dropped below 1.5 V were removed. The topography of the borehole wall might be such that impacts, and hence spikes, could repeat in the same location. Another possible source for the spikes in the formation itself are large dropstones composed of basalt or another rock type rich in magnetite. If they were close to the borehole wall, they could cause a repeatable spike in the magnetic field log. During logging at Hole 1095B, the metal caliper arm from the density logging tool broke off leaving metal debris in the hole during the GHMT run which would cause the same effect.

RELATIONSHIP OF THE FIELD IN THE BOREHOLE TO THE MAGNETIZATION OF THE SEDIMENT

The main aim of processing GHMT data is to derive the polarity of the remanent magnetization (J_r) of the sediment surrounding the borehole from the magnetic field intensity measured inside the borehole (B_0) (Fig. F3). (Strictly speaking, B is an induction, and the NMRS measures the induction by the field.)

The remanent magnetization of sediments is typically acquired during deposition by preferential alignment of the magnetic grains along the magnetic field direction. The sediment also carries an induced magnetization (J_i) along the direction of the present-day field. Both these magnetizations contribute to the field anomaly in the borehole (B_{fr} and B_{fi}), according to the following equations (Pozzi et al., 1988):

$$B_{frx} = (\mu_0/2)\, J_{rx} \quad (1)$$

and

$$B_{frz} = -\mu_0 \cdot J_{rz}, \quad (2)$$

(similarly for B_{fi}) where B_{frx} and B_{frz} are the components of B_{fr} in the x- (~north) and z- (down) directions.

The total field B_0 is much larger than the field anomaly caused by the remanent magnetization (in the example in Fig. F3; 44,000 nT compared to 114 nT), so B_0 and the Earth's field, B_r, are subparallel (to 0.104° in the Fig. F3 example). Therefore, to a very close approximation, it is the projection of the remanent anomaly B_{fr} along B_0 that contributes to the measured B_0. In the rest of this paper below this point, B_{fr} refers to the projection of the remanent anomaly along B_0. B_{fr} is calculated by (Pozzi et al., 1988):

$$B_{fr} = (\mu_0 J_r/2) \cdot (1 - 3\sin^2 I), \quad (3)$$

F3. Field geometry, Site 1096, p. 14.

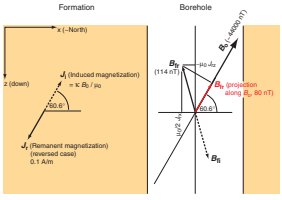

(similarly for B_{fi}) where I is the magnetic inclination. The field anomaly in the borehole B_{fi} caused by the induced magnetization J_i can be calculated from the above Equation 3. J_i itself can be calculated from the magnetic susceptibility κ, which is measured by the SUMS:

$$J_i = (B_0/\mu_0) \cdot \kappa, \quad (4)$$

where

$$B_0 = (\mu_0 \cdot H). \quad (5)$$

In the above equations (see, for example, Parkinson, 1983),

- B = magnetic induction (units = tesla [T]; 1 nT = 10^{-9} T);
- H = magnetic field (units = A/m);
- J = magnetization, volume normalized (units = A/m);
- κ = magnetic susceptibility, volume normalized (unitless; presented here in $\times 10^{-6}$ SI units); and
- μ_0 = permeability of nonmagnetic material = $4\pi \times 10^{-7}$ (in SI units).

DETERMINATION OF THE REMANENT ANOMALY

The remanent anomaly (B_{fr}) is the field in the borehole caused by remanent magnetization of the sediment, projected along B_0 (Fig. F3). B_{fr} is determined by subtracting the other individual fields that contribute to the total field measurement B_0:

$$B_0(z,t) = B_r(z) + B_a(z) + B_{fr}(z) + B_{fi}(z) + B_t(z,t). \quad (6)$$

All the components of B_0 are a function of depth (z). The time-dependant magnetic field (B_t), generated in the ionosphere, also contributes.

B_r, the field generated in the Earth's core, forms the largest component of B_0 by about two orders of magnitude. It is estimated from the International Geomagnetic Reference Field (IGRF) (Table T1).

B_a is the regional magnetic field (seafloor and other crustal anomalies). The field caused by the metal (magnetic) drill pipe (B_{pipe}) is also included within B_a. It decays with distance (r) away from the pipe ($B_{pipe} = a/r^3$). The pipe effect is determined by iterative forward modeling until a satisfactory fit to the data is obtained. The pipe effect for Holes 1096C and 1095B is shown in Figures F4 and F5.

B_t, the time dependant field, is generally neglected. Two passes of the GHMT were run so that the repeatability could be checked. Generally the differences were slight and could be neglected. The "spikes" in the Hole 1095B magnetic field log can be considered to be part of B_t, and they have been removed from the log where the tool voltage falls below 1.5 V (Fig. F5).

B_{fi}, the induced field anomaly, is calculated using Equations 3, 4, and 5, with values for B and I taken from the IGRF values for the site (Table T1).

There is some uncertainty in the values of the component fields. For example, B_r changes with time and depth. A major uncertainty is in the part of B_a due to local crustal anomalies, which is the main reason the GHMT average field value differs from the IGRF value (Table T1).

T1. IGRF field values for the logged Leg 178 sites, p. 22.

F4. The original total field (B_0) and susceptibility (κ) logs, Hole 1096C, p. 15.

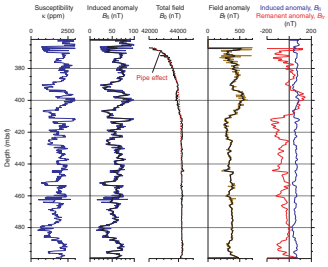

F5. The original total field (B_0) and susceptibility (κ) logs, Hole 1095B, p. 16.

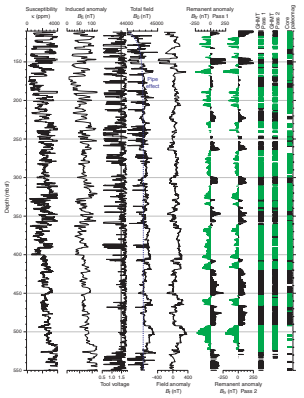

Hence, after B_r, B_a, and B_{fi} have been subtracted from the measured total field B_0 to leave B_{fr}, the result can be offset from zero by a few hundred nT. However, we know that for a mixed polarity sequence the remanent field anomaly (B_{fr}) will average out to near zero, and therefore we can correct for the offset. For Hole 1095B, a linear fit was subtracted from the B_{fr} curve to give a corrected B_{fr} curve. For Hole 1096C, a constant value was subtracted (395 nT) (a linear fit was not appropriate for this hole because the logged interval contains essentially only one normal and one reversed polarity zone). The corrected B_{fr} curves are shown in Figures **F4** and **F5**, along with the uncorrected field anomaly B_f (= B_{fi} + B_{fr}) and the original B_0 and κ logs. For Hole 1095B, the remanent anomalies for the two passes of the GHMT tool were calculated independently and are similar (Fig. **F5**).

CORRELATION ANALYSIS TO DETERMINE POLARITY

An alternative way to overcome the problem of uncertainty in the values of the component fields is to employ a processing method referred to as correlation analysis (Vibert-Charbonnel, 1996; Louvel and Galbrun, 2000). The principle employed by the correlation analysis method (Pozzi et al., 1993) is illustrated in Figure **F6.** Both J_r and J_i are dependant on the concentration of ferrimagnetic minerals in the sediment, and this concentration varies. J_r and J_i correlate in normal polarity intervals, and the linear regression line has a positive gradient; whereas, in reversed polarity intervals, J_r is inversely correlated with J_i, and the linear regression line has a negative gradient. The same applies to B_{fr} and B_{fi} on which the correlation analyses are actually performed. The linear regressions are applied to successive depth intervals ("windows") of various thickness (1.5-, 2.5-, 4.5-, 8-, and 13-m windows are presented here). Linear regressions with a correlation coefficient <0.5 are not plotted in the results (Figs. **F7, F8**). Prior to the correlation analyses, B_{fr} and B_{fi} are smoothed with an 11-sample (1.5 m) Hanning filter, so that the two measurements have comparable vertical resolution.

Some preconditions are necessary for this method to work well. First, the susceptibility of the formation must vary so that log features exist to correlate/anticorrelate. This is not usually a problem. Second, the remanent magnetization must be subparallel to the induced magnetization. This might not be the case in older strata whose position relative to the magnetic poles has changed as a result of plate motions. Third, it is assumed that the absolute ratio of the remanent to the induced magnetizations is constant. In fact, the remanent intensity depends on the type of sediment and the magnetic field intensity at the time of deposition as well as the ferrimagnetic mineral concentration (e.g., Tauxe, 1993, Williams et al., 1998). However, a change in this ratio will affect only the gradient of the linear regression, not its polarity. Fourth, since the peaks and troughs of the remanent and induced anomalies can be quite short (e.g., 1 m), the depth accuracy of the logs becomes important; if the peaks and troughs are not in phase, the correlation analysis will be disturbed. The SUMS takes measurements at a horizon some time before the NMRS (because it is higher up the tool string and the log is taken in the upward direction), and the ship's heave is never entirely removed from the tool motion resulting in (usually slight) depth

F6. Remanent (B_{fr}) vs. induced (B_{fi}) anomalies, Hole 1096C, p. 17.

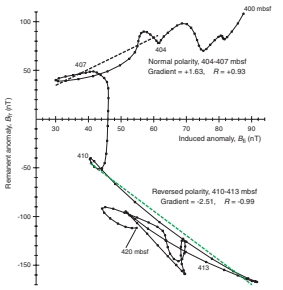

F7. Polarity determined by correlation analysis, Hole 1096C, p. 18.

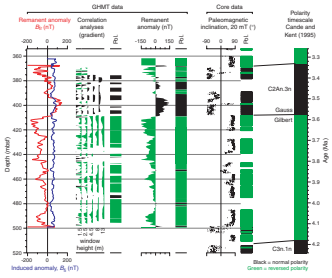

F8. Polarity determined by correlation analysis, Hole 1095B, p. 19.

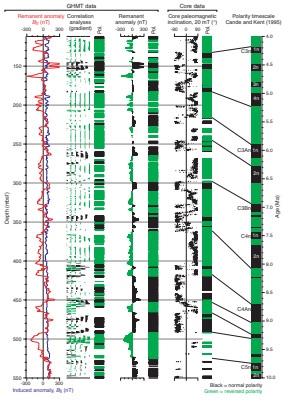

offsets. Tool heave was especially significant in Hole 1095B (Fig. F2). Fifth, the magnetic induction logs from Hole 1095B contain spikes. We have removed these spikes and linearly interpolated values into the gaps left behind; however, the correlations from intervals where there were spikes cannot be confidently relied on. The fourth and fifth items are principally responsible for the inaccuracies in the results of the correlation analysis for Hole 1095B.

POLARITY RESULTS

Hole 1096C

In Hole 1096, the polarity sequence derived from the GHMT is quite simple (Fig. F7), with predominantly normal polarity from 375–408 meters below seafloor (mbsf) and predominantly reversed polarity <408 mbsf. The polarity of the remanent induction is in general agreement with the polarity from the correlation analyses. Both agree with the core paleomagnetic polarity.

The major difference is at the top of the logged section (367–375 mbsf), where both the GHMT methods indicate reversed polarity, whereas the core is normally magnetized. This is almost certainly because of proximity to the metal drill pipe and incomplete removal of its magnetic field, giving lower than expected remanent induction values.

Hole 1095B

The logged section of Hole 1095B represents a longer time interval than the section in Hole 1096C, so the polarity sequence is more complex (Fig. F8). The polarity of the remanent induction shows some agreement with the polarity from the correlation analyses. However, the latter is only about 50% complete because of the cutoff of $R = 0.5$ in the correlation analyses; it is strongly affected by depth mismatch between B_{fr} and B_{fi} and by the presence of spikes.

The polarity of the remanent induction mostly agrees with the core paleomagnetic polarity (Figs. F5, F8). As with Hole 1096C, there is some disagreement at the top of the logged section near the pipe. The shipboard interpretation of the magnetic polarity data is indicated in Figure F8 (Barker, Camerlenghi, Acton, et al., 1999). Other interpretations are possible, and the combined magneto- and biostratigraphy of Site 1095 are presented and discussed elsewhere in this volume.

CORE-LOG COMPARISON

Magnetic susceptibility is a property that is measured both on core and downhole. Remanent magnetization is measured on core and can be derived from the downhole magnetic field and susceptibility data. Comparison of the log to the core data offers insights into the advantages and limitations of both data sets, and, in particular, an assessment can be made of the sediment magnetization both before and after the drill string overprint has been imparted to the cores.

Differences in depth positioning of the cores and logs are due to ship heave, tides, inaccurate determination of the depth to seafloor, incomplete core recovery, core expansion, and so forth. On the basis of matching polarity intervals, a bulk depth shift (downward) of 6 m has

been applied to the Hole 1095B core data and of 3 m to the Hole 1096C core data. There are some small variations in the depth offset downhole, but the bulk depth shifts applied here are typically good enough to bring the different data sets to within 1 m of each other.

Susceptibility

Both the Bartington core susceptibility system and the SUMS logging tool work on the same principle. They contain a transmitter coil that creates an alternating magnetic field, which induces a magnetization that is proportional to the susceptibility of the sediment. The frequency of the two systems are similar: 220 Hz for the SUMS and 565 Hz for the Bartington meter. The Bartington meter output unit is ~10^{-5} SI units, and the SUMS output unit is "ppm SI" equivalent to about 10^{-6} SI units. Both units are volume normalized. The volume measured by the SUMS is much larger than that measured by the Bartington meter. The vertical resolution of the SUMS is about 40 cm, and the depth of investigation is about 80 cm (Vibert-Charbonnel, 1996).

The overall shape of the two curves is similar (Fig. F9); however, differences in amplitude are significant and are attributed to difficulties in volume normalization. The range of variation is greater for the core susceptibility, which may be due to the variable thickness of core, especially in the extended core barrel cores.

F9. Comparison of the core and log measurements, Hole 1096C, p. 20.

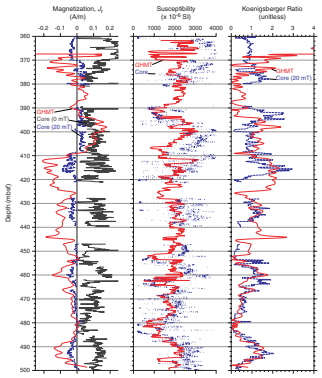

Magnetization

The remanent magnetization (J_r) of the sediment can be calculated from the GHMT remanent anomaly (B_{fr}) using Equation 3 (see "Relationship of the Field in the Borehole to the Magnetization of the Sediment," p. 3). This magnetization has uncertainties due to the possibly incomplete removal of the other components that make up the (measured) total field, to variations in hole diameter, and to uncertainties in the volume of sediment measured.

The shipboard cryogenic magnetometer was used to measure the magnetization of split cores (Barker, Camerlenghi, Acton et al., 1999). The initial core magnetization was measured, followed by the magnetization remaining after 20- and 30-mT alternating-field (AF) demagnetization. The cores acquire a drill string overprint during coring and their trip up the pipe to the ship. The overprint is commonly directed vertically downward (e.g., Roberts et al., 1996). The cores have no induced magnetization because they are measured within shielding that creates a very low field environment.

The magnitude of the magnetization is similar to, or sometimes slightly lower than, the initial core magnetization (Fig. F9). However, whereas the core magnetization is always in the downward direction because of the overprint, the in situ magnetization derived from the GHMT logs shows both normal and reversed polarity. The core magnetization after the 20-mT demagnetization step is of lower magnitude than the in situ magnetization, but the two curves have generally the same shape.

We interpret these observations to mean that the drill string magnetization replaces the low-coercivity remanent magnetization in the cored sediment and does not significantly affect the higher-coercivity components. The drill string effect does not extend as strongly into the sediment surrounding the borehole, leaving the in situ magnetization

largely intact. A unidirectional overprint would manifest itself in the GHMT-derived magnetization as a reduction in amplitude without a change in the polarity, because the remanent anomaly derived from the GHMT total field log is set so that there are both positive and negative values. The generally good agreement of the polarity determinations from cores and logs shows that the remanent component of the field has been well isolated.

Koenigsberger Ratio

The Koenigsberger ratio is the ratio of the remanent to the induced magnetization. Its value depends on two main factors: the type of sediment and the paleointensity of the Earth's magnetic field. The dependence on sediment type is caused in large part by the grain size. Larger (multidomain) magnetic grains have a smaller magnetization per volume than smaller (pseudo–single domain) grains and are less able to overcome mechanical resistance from the surrounding matrix and align along the magnetic field. Hence, a sediment containing predominantly large ferrimagnetic grains will have a smaller remanence than one containing smaller grains. Lithic clasts that contain magnetic grains are even more unlikely to be able to align along the magnetic field, a situation that is likely to apply to diamict sediments. Because the susceptibility, and hence induced magnetization, is fairly constant with magnetite grain size (Heider et al., 1996), the Koenigsberger ratio should also be smaller for coarser-grained sediments. The ratio also depends on paleointensity because an increased intensity of the Earth's field leads to better alignment of magnetic grains along it and therefore an increased remanent magnetization. This is demonstrated in independent sediment sections that record similar paleointensity variations through time (e.g., Guyodo and Valet, 1996), although there are still doubts about the completeness of the normalization techniques (e.g., Kok, 1999).

The Koenigsberger ratios derived in this way are only approximate because of the uncertainties in the remanent magnetization and susceptibility. The ratio cannot be calculated absolutely from the core measurements, because of the large overprint and subsequent demagnetization. However, the shapes of the log-based ratio and the ratio of the 20-mT demagnetization step to the core susceptibility are found to be reasonably similar below 400 mbsf in Hole 1096C.

EFFICIENCY OF PALEOMAGNETIC RECORDING AT DIFFERENT SITES

Comparison of the Koenigsberger ratio averaged over time in different sediment types can shed light on the paleomagnetic recording efficiency of those sediment types. The contribution of the geomagnetic paleointensity to the ratio is assumed here to be averaged out over the examined interval. This is likely to be a good first order approximation as the paleointensity varies at a scale of thousands to tens or hundreds of thousands of years, and the intervals examined are typically over a million years.

Time-averaged Koenigsberger ratios for eight ODP sites are given in Table **T2** and Figure **F10.** The time-averaged Koenigsberger ratio is calculated quite easily from the GHMT logs: the mean absolute value for

T2. Koenigsberger ratios derived from GHMT logs for a selection of ODP sites, p. 23.

F10. Comparison of time-averaged Koenigsberger ratios, p. 21.

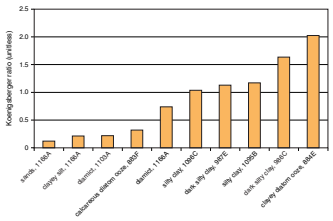

the remanent anomaly and the mean value of the induced anomaly are calculated and their ratio is taken. We attempted to select log intervals of the same sediment type for this analysis (Table T2). To enable comparison, the ratios have been corrected for latitude, by assuming the geomagnetic paleointensity at the surface is due to an axial dipole.

The ratios for the silty clays from Holes 1095B and 1096C are similar to each other but about five times as large as for the diamict of Hole 1103A on the continental shelf. The diamict logged in Leg 188 Hole 1166A (Prydz Bay) (O'Brien, Cooper, Richter, et al., 2000) has a similarly low ratio. The glacial and preglacial coarse-grained sediments at Site 1166 also have low ratios. The silty clays of Deep Sea Drilling Project (DSDP) Leg 162 Hole 987E have values comparable to the silty clays logged during Leg 178. Hole 986C has a high ratio of 1.6 (no core paleomagnetic results were obtained from this hole, because a strong drill string overprint). Both these DSDP Leg 162 holes yielded good GHMT polarity stratigraphies by the correlation analysis method (Higgins et al., 1999). DSDP Leg 145, Hole 884E has the highest ratio of the examined holes, at 2.02. GHMT logs from this hole gave an excellent polarity stratigraphy (Thibal et al., 1995).

The main result is that finer-grained sediments have higher Koenigsberger ratios than coarser-grained sediments, with the implication that the finer-grained sediments record the paleofield more efficiently. This result is expected, given the known mechanism of depositional remanence acquisition described above. This result partly explains why it was difficult to establish a polarity stratigraphy for Hole 1103A. The other reasons were the presence of numerous spikes in the record, the depositional environment, and the lack of a priori biostratigraphic dates.

The Koenigsberger results are also important from the point of view of paleointensity studies, in which it is important to establish that the paleomagnetic recording efficiency does not change significantly down the section under study. This is checked by establishing that the magnetic mineral type and size fall within a certain range (e.g., Tauxe, 1993). The remanence intensity normalized by some measure of ferrimagnetic mineral concentration (e.g., susceptibility) can then be taken to be a measure of the field paleointensity.

The ratios presented here vary by a factor of ~10, depending on the sediment type. This is likely because a larger average ferrimagnetic grain size leads to less efficient paleomagnetic recording. Ratios from just the fine-grained sediment types are more constant, varying by a factor of ~2. Paleointensity records are usually generated from this kind of fine-grained sediment, and this study offers background information about the variability of the paleomagnetic recording efficiency. It is important that the recording efficiency is as constant as possible in the particular sediment interval under study. More determinations of the Koenigsberger ratio from different sites will be useful to add weight to these initial analyses.

CONCLUSIONS

The general agreement of the GHMT polarities to the core paleomagnetic polarities demonstrates that, in broad terms, the GHMT polarities for the Leg 178 sediment drift sites are valid and may be used to complement the core results and for age interpretation in intervals where core was not recovered.

The sediment magnetization derived from the GHMT logs has a similar absolute value to the core magnetization before AF demagnetization; however, the GHMT results indicate that the sediment surrounding the borehole has not suffered a significant drill string overprint, unlike the core.

Comparison of time averaged Koenigsberger ratios in different sediment types shows that silty clays (from sediment drifts) have a fairly consistent paleomagnetic recording efficiency, whereas coarser-grained sediments can be less efficient by up to a factor of 10 than the silty clays.

REFERENCES

Barker, P.F., Camerlenghi, A., Acton, G.D., et al., 1999. *Proc. ODP, Init. Repts.,* 178 [CD-ROM]. Available from: Ocean Drilling Program, Texas A&M University, College Station, TX 77845-9547, U.S.A.

Cande, S.C., and Kent, D.V., 1995. Revised calibration of the geomagnetic polarity timescale for the Late Cretaceous and Cenozoic. *J. Geophys. Res.,* 100:6093–6095.

Guyodo, Y., and Valet, J.-P., 1996. Relative variations in geomagnetic intensity from sedimentary records: the past 200,000 years. *Earth Planet. Sci. Lett.,* 143:23–36.

Heider, F., Zitzelberger, A., and Fabian, K., 1996. Magnetic susceptibility and remanent coercive force in grown magnetite crystals from 0.1 µm to 6 mm. *Phys. Earth Planet. Inter.,* 93:239–256.

Higgins, S.M., Kreitz, S., King, T., and Goldberg, D., 1999. Data report: Magnetic polarity and susceptibility measurements from the geological high-resolution magnetometer tool at Sites 984, 986, and 987. *In* Raymo, M.E., Jansen, E., Blum, P., and Herbert, T.D. (Eds.), 1999. *Proc. ODP, Sci. Results,* 162: College Station, TX (Ocean Drilling Program), 265–269.

Kok, Y.S., 1999. Climatic influence in NRM and ^{10}Be-derived geomagnetic paleointensity data. *Earth Planet. Sci. Lett.,* 166:105–119.

Louvel, V., and Galbrun, B., 2000. Magnetic polarity sequences from downhole measurements in ODP Holes 998B and 1001A, Leg 165, Caribbean Sea. *Mar. Geophys. Res.,* 21:561–577.

O'Brien, P.E., Cooper, A.K., Richter, C., et al., 2001. *Proc. ODP, Init. Repts.,* 188 [CD-ROM]. Available from: Ocean Drilling Program, Texas A&M University, College Station, TX 77845-9547, USA.

Parkinson, W.D., 1983. *Introduction to Geomagnetism:* Edinburgh (Scottish Academic Press).

Pozzi, J.-P., Barthés, V., Thibal, J., Pocachard, J., Lim, M., Thomas, T., and Pagès, G., 1993. Downhole magnetostratigraphy in sediments: comparison with the paleomagnetism of a core. *J. Geophys. Res.,* 98:7939–7957.

Pozzi, J.-P., Martin, J.P., Pocachard, J., Feinberg, H., and Galdeano, A., 1988. In situ magnetostratigraphy: interpretation of magnetic logging in sediments. *Earth Planet. Sci. Lett.,* 88:357–373.

Roberts, A.P., Stoner, J.S., and Richter, C., 1996. Coring-induced magnetic overprints and limitations of the long-core paleomagnetic measurement technique: some observations from Leg 160, eastern Mediterranean Sea. *In* Emeis, K.-C., Robertson, A.H.F., Richter, C., et al., *Proc. ODP, Init. Repts.,* 160: College Station, TX (Ocean Drilling Program), 497–505.

Roperch, P., Barthès, V., Pocachard, J., Collot, J.-Y., and Chabernaud, T., 1994. Magnetic logging and in-situ magnetostratigraphy: a field test. *In* Greene, H.G., Collot, J.-Y., Stokking, L.B., et al., *Proc. ODP, Sci. Results,* 134: College Station, TX (Ocean Drilling Program), 577–589.

Tauxe, L., 1993. Sedimentary records of relative paleointensity of the geomagnetic field: theory and practice. *Rev. Geophys.,* 31:319–354.

Thibal, J., Pozzi, J.-P., Barthés, V., and Dubuisson, G., 1995. Continuous record of geomagnetic field intensity between 4.7 and 2.7 Ma from downhole measurements. *Earth Planet. Sci. Lett.,* 136:541–550.

Vibert-Charbonnel, P., 1996. Methodes de traitment des mesures magnetiques en forage pour la datation haute-resolution des series sedimentaires. [Thesis]. L'Institute National Polytechnique de Grenoble.

Williams, T., Thouveny, N., and Creer, K.M., 1998. A normalised intensity record from Lac du Bouchet: geomagnetic paleointensity for the last 300 kyr? *Earth Planet. Sci. Lett.,* 156:33–46.

Figure F1. Bathymetric map of the West Antarctic Peninsula area, Leg 178. Red dots = drill sites, D1–D7 = sediment drifts.

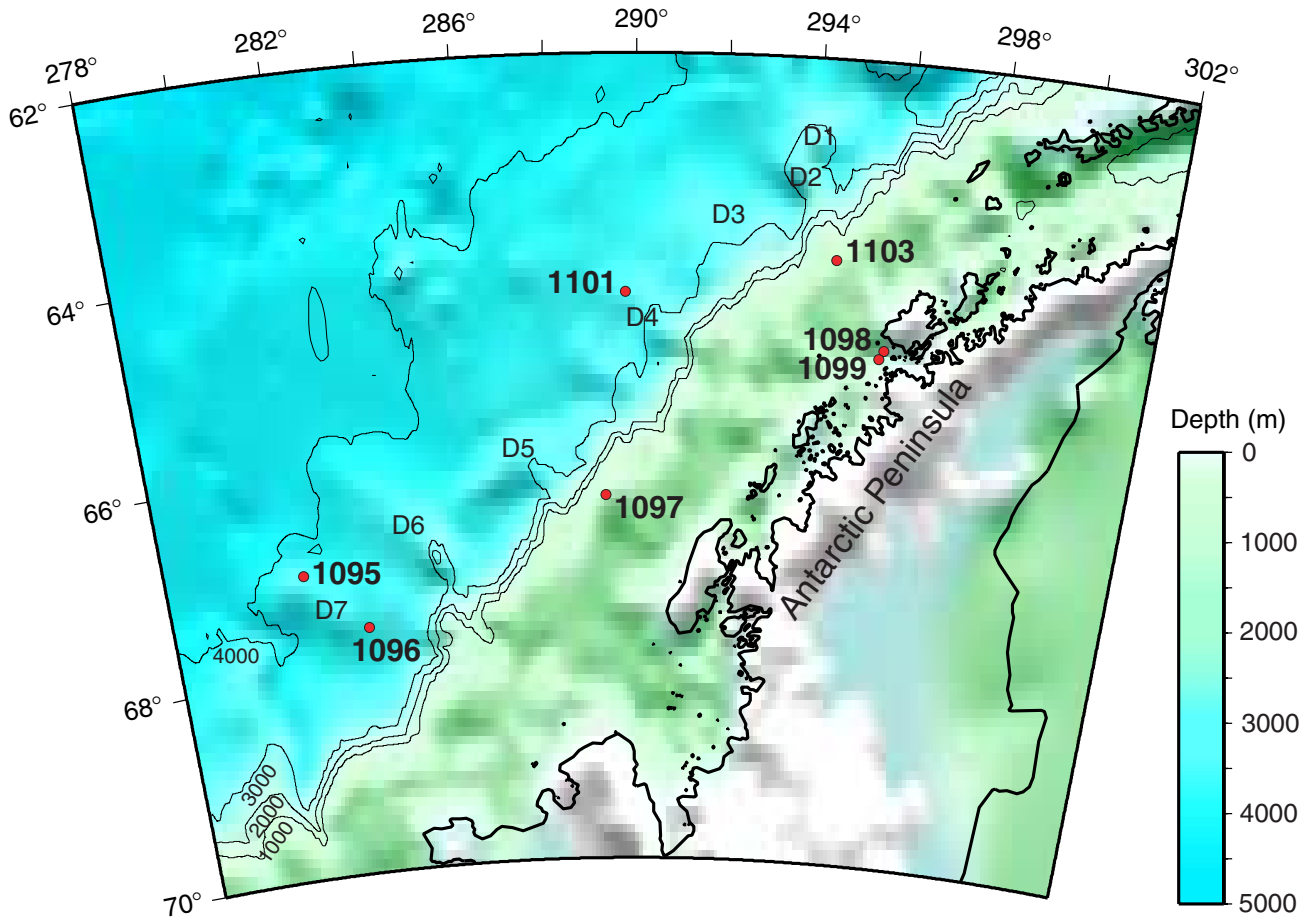

Figure F2. Comparison of the two passes of the GHMT over 80-m sections in Holes 1095B and 1096C. Notice the greater repeatability and near absence of spikes in Hole 1096C compared with Hole 1095B. Solid lines = Pass 1, dashed lines = Pass 2.

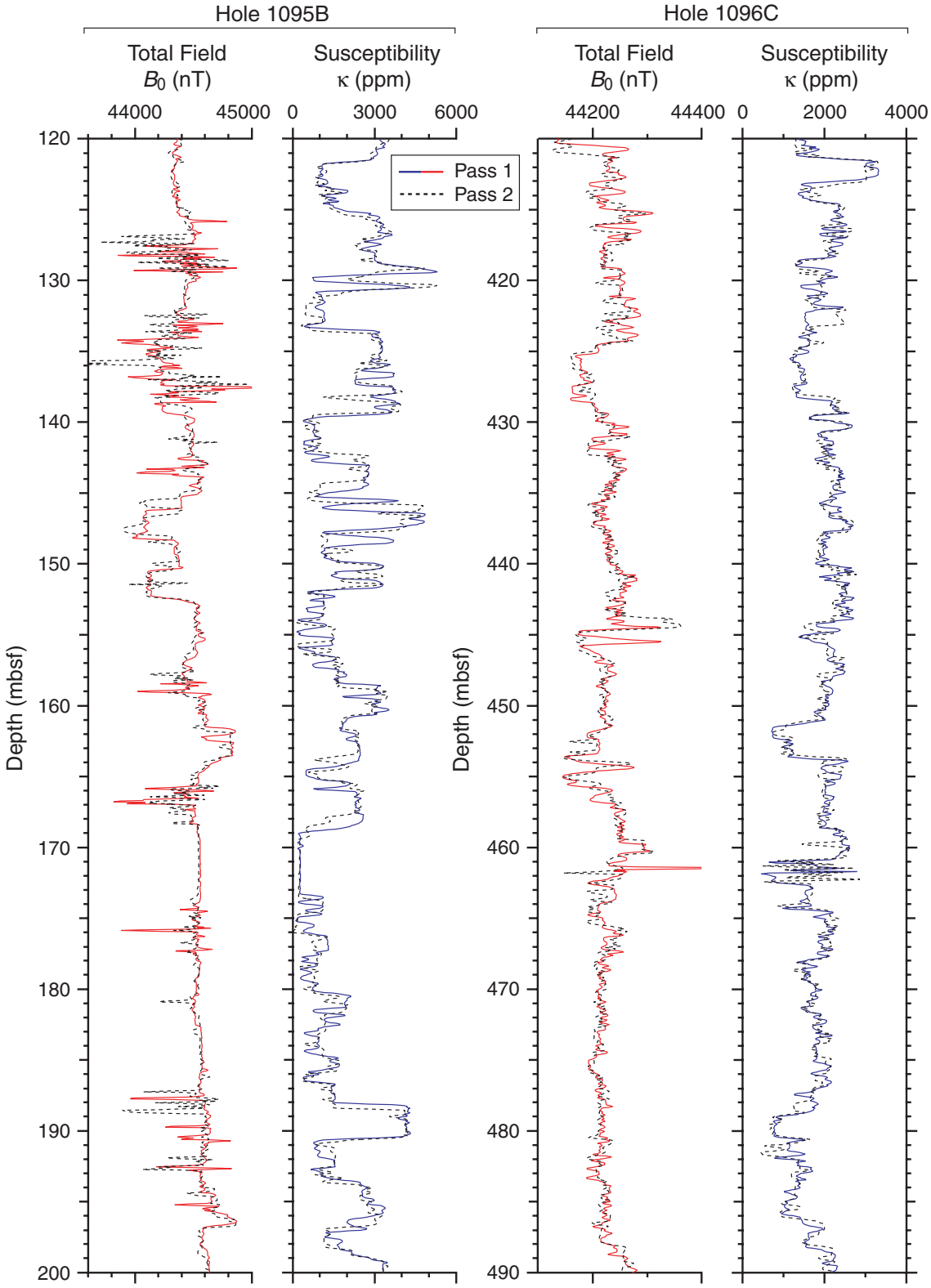

Figure F3. Field geometry at Site 1096, showing the remanent and induced magnetizations (J_r and J_i) in the formation and the remanent and induced field anomalies they cause in the borehole (B_{fr} and B_{fi}). Given a sediment magnetization (J_r) of 0.1 A/m, the observed anomaly in the borehole (B_{fr}) is 80 nT (see **"Relationship of the Field in the Borehole to the Magnetization of the Sediment,"** p. 3). Note that the fields in the borehole do not have the same direction as the sediment magnetizations that produce them. This can be verified in the actual data: for example, below 409 mbsf in Hole 1096C, the sediment has a reverse magnetization and the anomaly in the total field log is positive (Fig. **F4,** p. 15, middle graph).

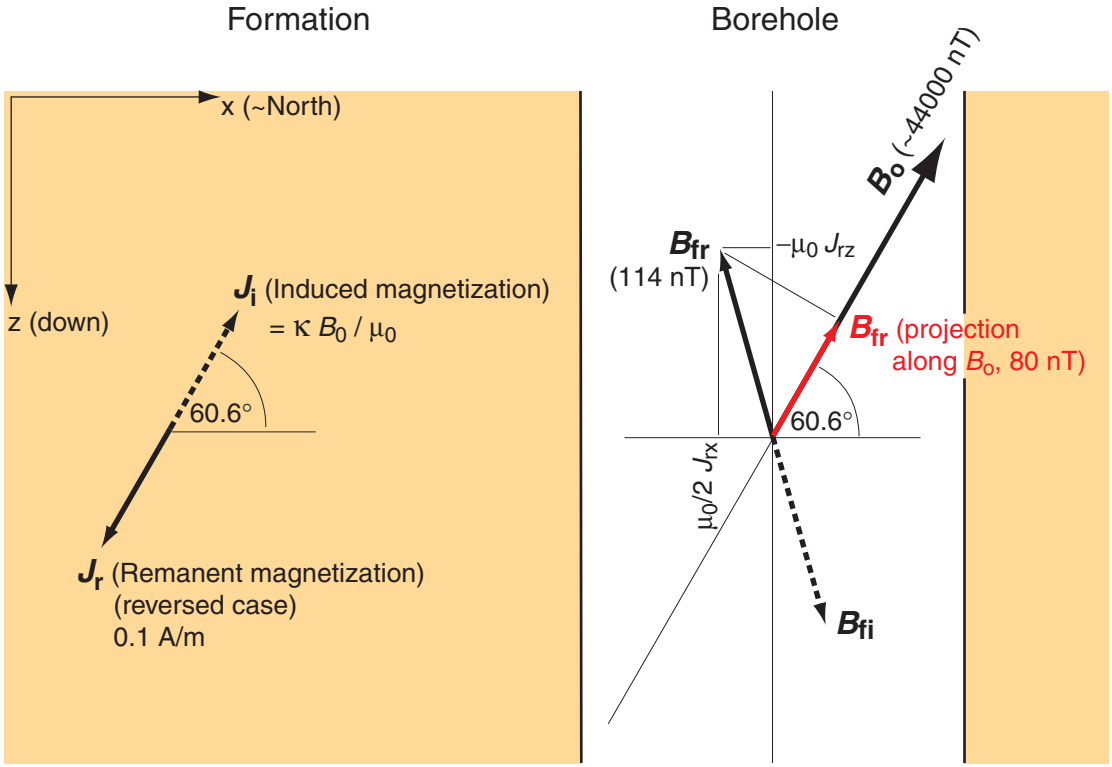

Figure F4. The original total field (B_0) and susceptibility (κ) logs for Hole 1096C and the remanent and induced borehole field anomalies derived from them. The background field value and the pipe effect are subtracted from the measured B_0 to leave B_f. B_{fi} is subtracted from B_f to leave B_{fr}, the anomaly caused by the sediment's remanent magnetization.

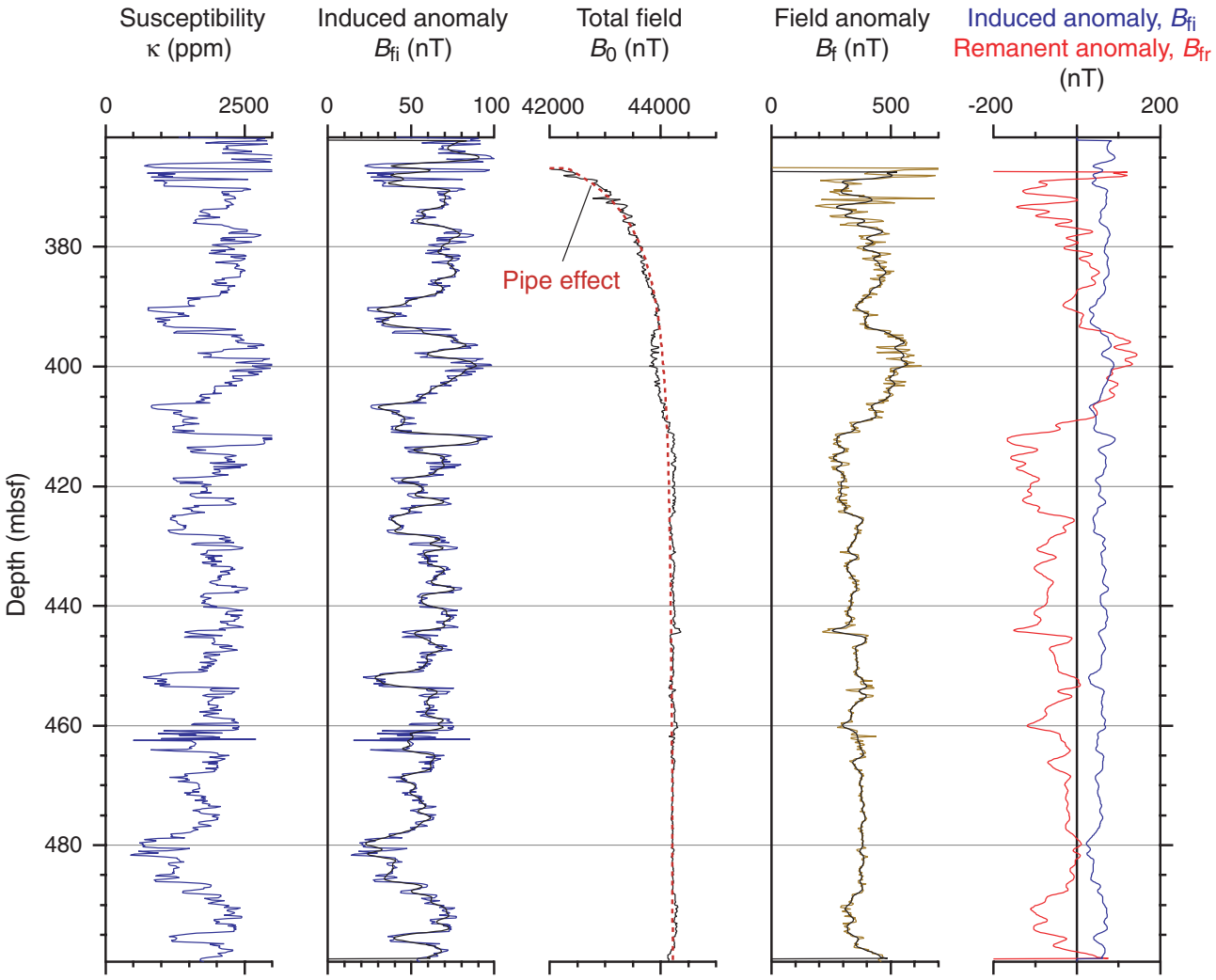

Figure F5. The original total field (B_0) and susceptibility (κ) logs for Hole 1095B and the remanent and induced borehole field anomalies derived from them. The background field value and the pipe effect are subtracted from the measured B_0 to leave B_f. B_{fi} is subtracted from B_f to leave B_{fr}, the anomaly caused by the sediment's remanent magnetization. The results from the two passes of the geological high-resolution magnetic tool (GHMT) were computed independently and are plotted alongside the core paleomagnetic results for the 20-mT AF demagnetization step.

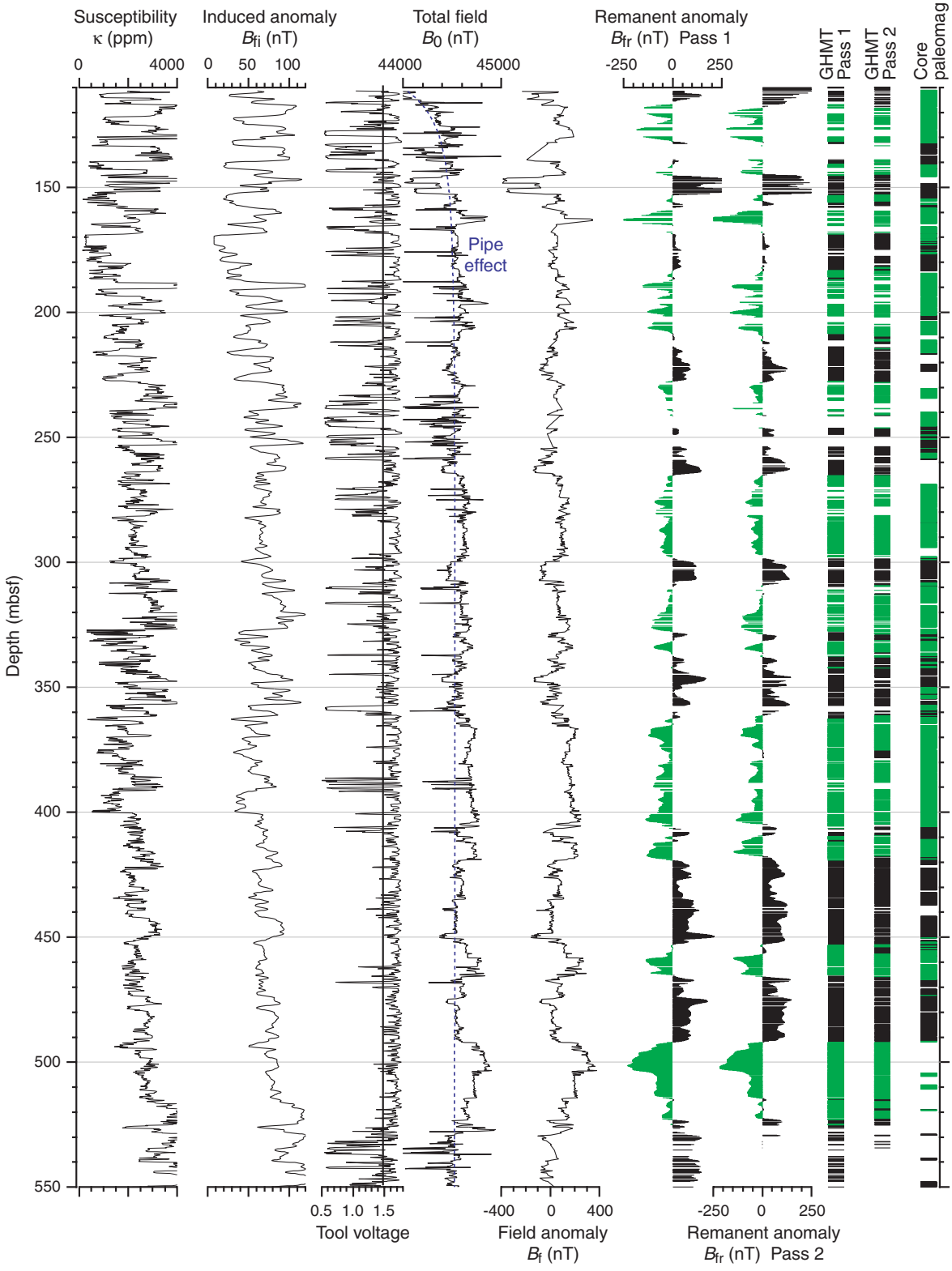

Figure F6. Remanent (B_{fr}) vs. induced (B_{fi}) anomalies for the interval from 400 to 420 mbsf in Hole 1096C, covering the Gilbert-Gauss polarity reversal, illustrating the principles of the correlation analysis method. Correlation between B_{fr} and B_{fi} indicates normal polarity, and anticorrelation indicates reversed polarity.

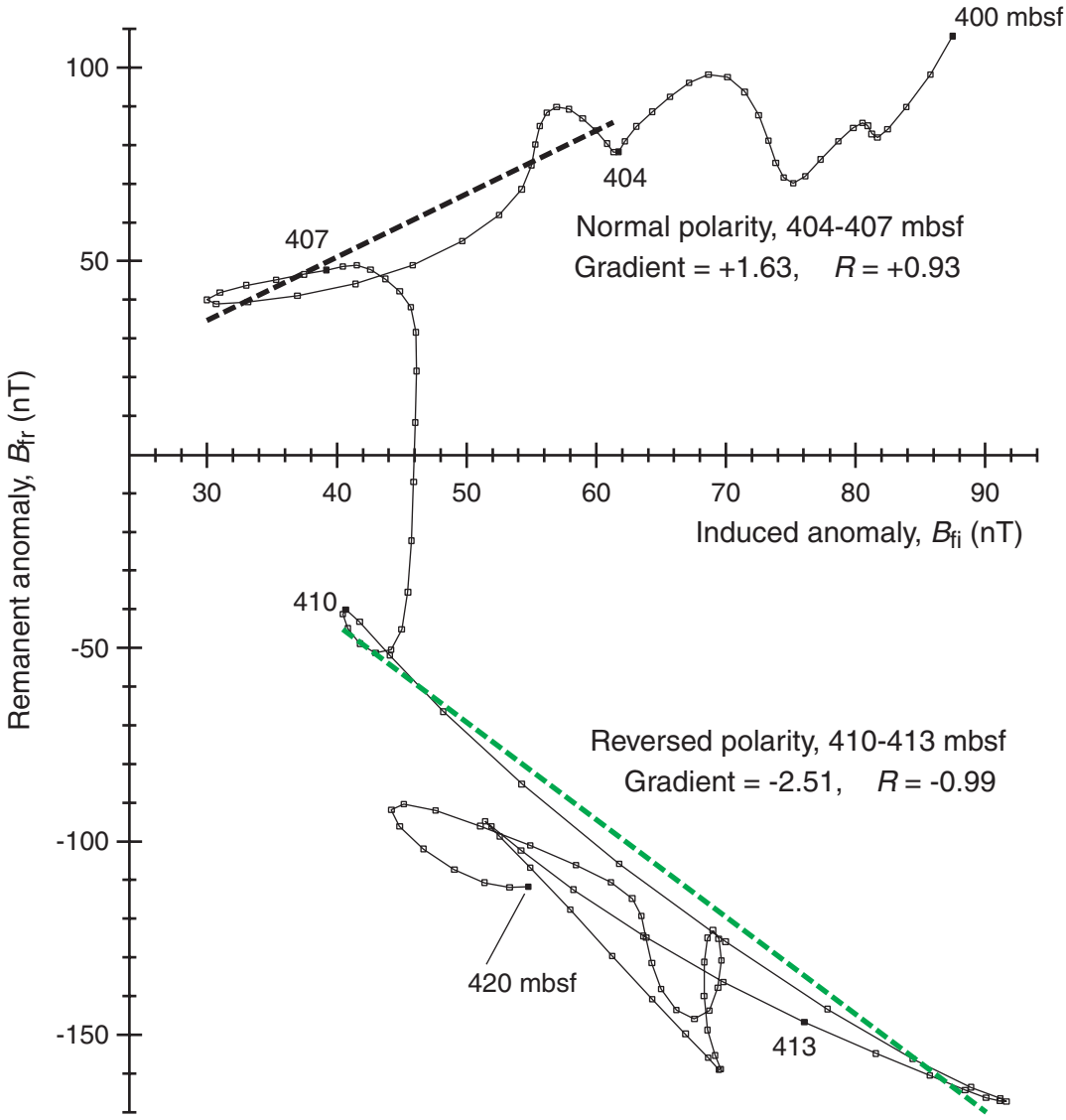

Figure F7. Polarity determined at Hole 1096C by correlation analysis, by the sign of the remanent anomaly, and by the inclination of the core paleomagnetic vector after AF demagnetization at 20 mT. In each case, a polarity column is given: black = normal polarity, green = reversed polarity, and white = undetermined polarity. The depth interval employed in the correlation analyses are 1.5, 2.5, 4.5, 8, and 13 m. The shipboard interpretation of the polarity stratigraphy (Barker, Camerlenghi, Acton, et al., 1999) is presented. GHMT = geological high-resolution magnetic tool.

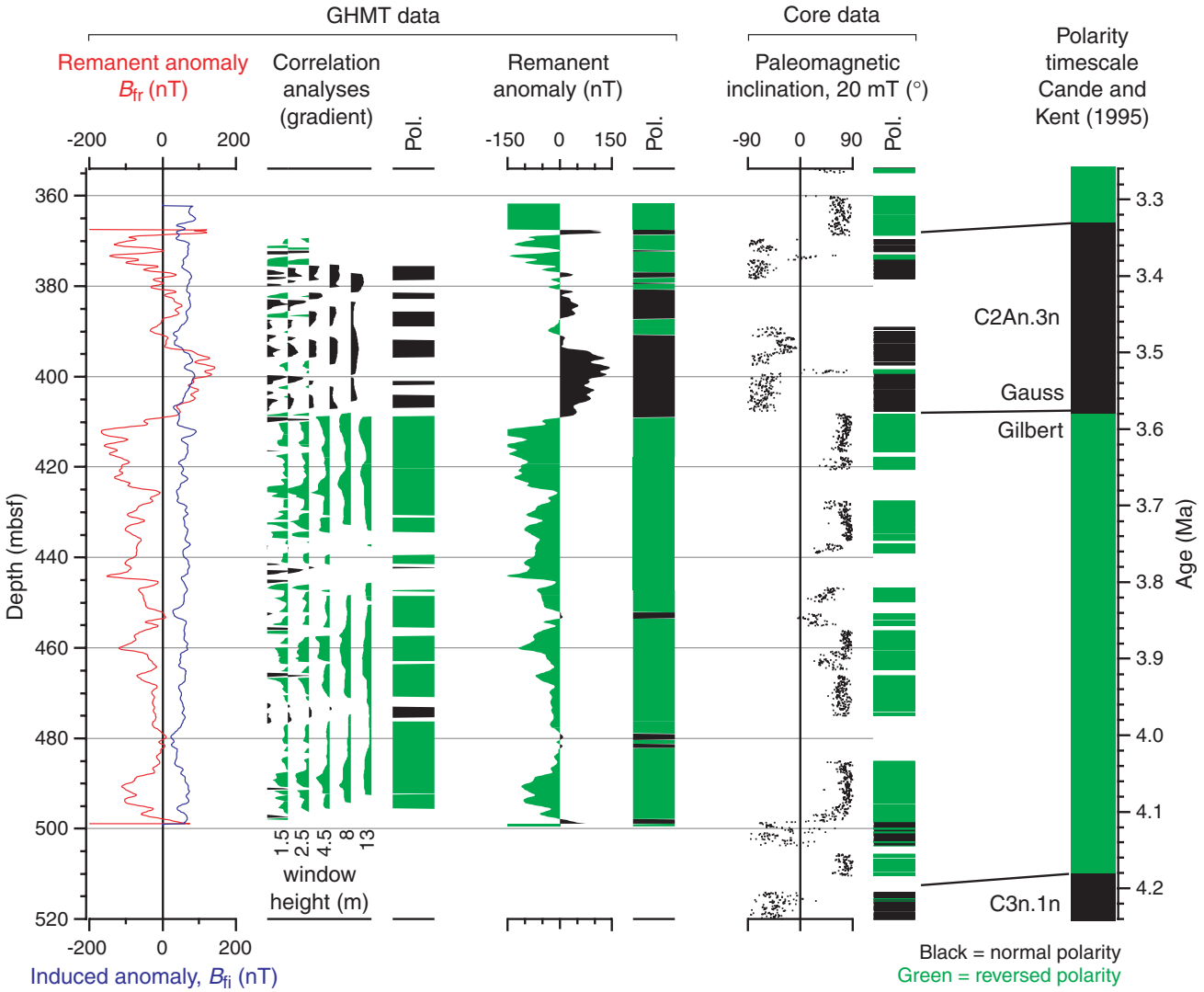

Figure F8. Polarity determined at Hole 1095B by correlation analysis, by the sign of the remanent anomaly, and by the inclination of the core paleomagnetic vector after AF demagnetization at 20 mT. In each case, a polarity column is given: black = normal polarity, green = reversed polarity, and white = undetermined polarity. The depth interval employed in the correlation analyses are (from left) 1.5, 2.5, 4.5, 8, and 13 m. The shipboard interpretation of the polarity stratigraphy (Barker, Camerlenghi, Acton, et al., 1999) is presented. GHMT = geological high-resolution magnetic tool.

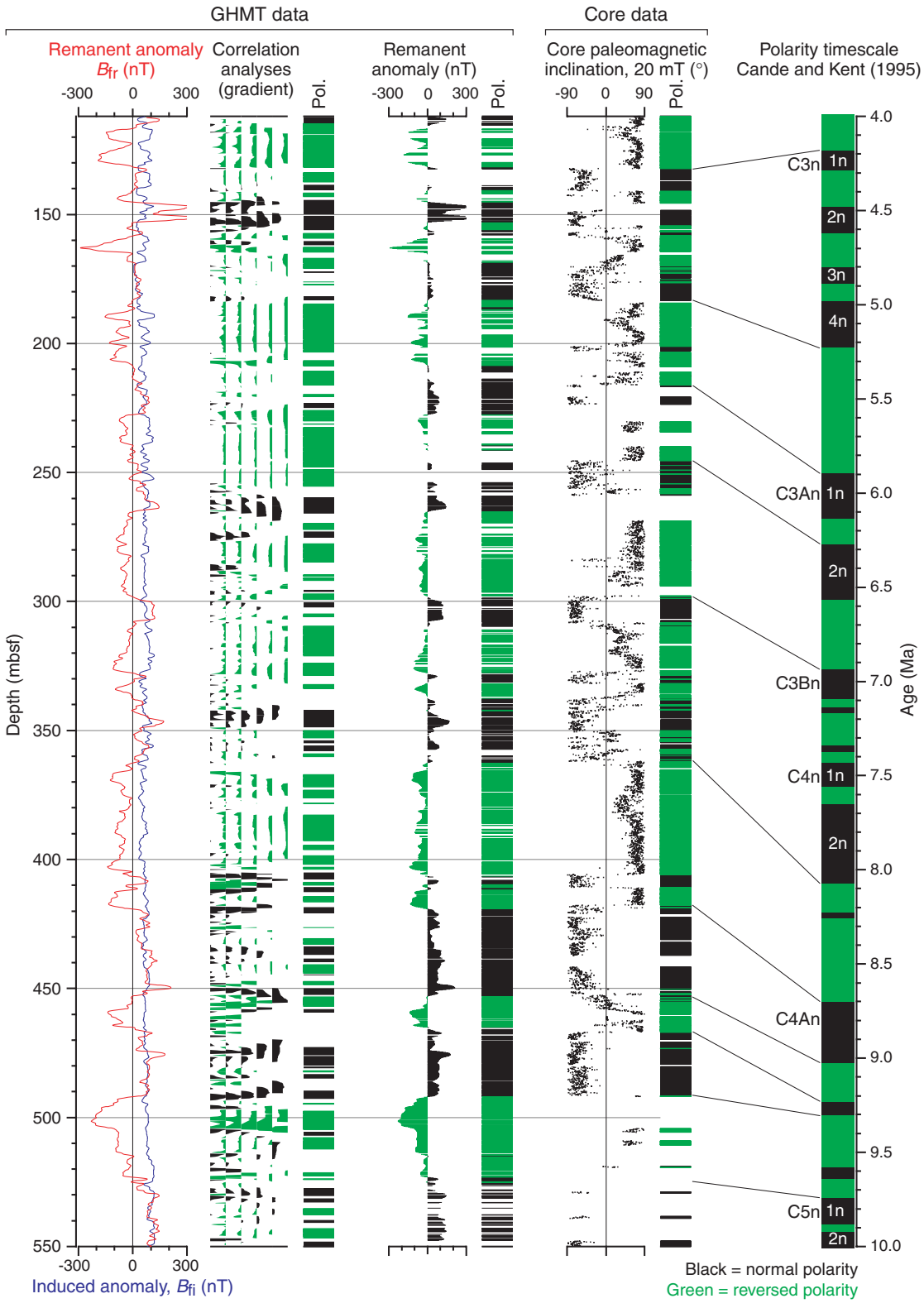

Figure F9. Comparison of the core and log measurements of sediment magnetization intensity, susceptibility, and Koenigsberger ratio from Hole 1096C. GHMT = geological high-resolution magnetic tool.

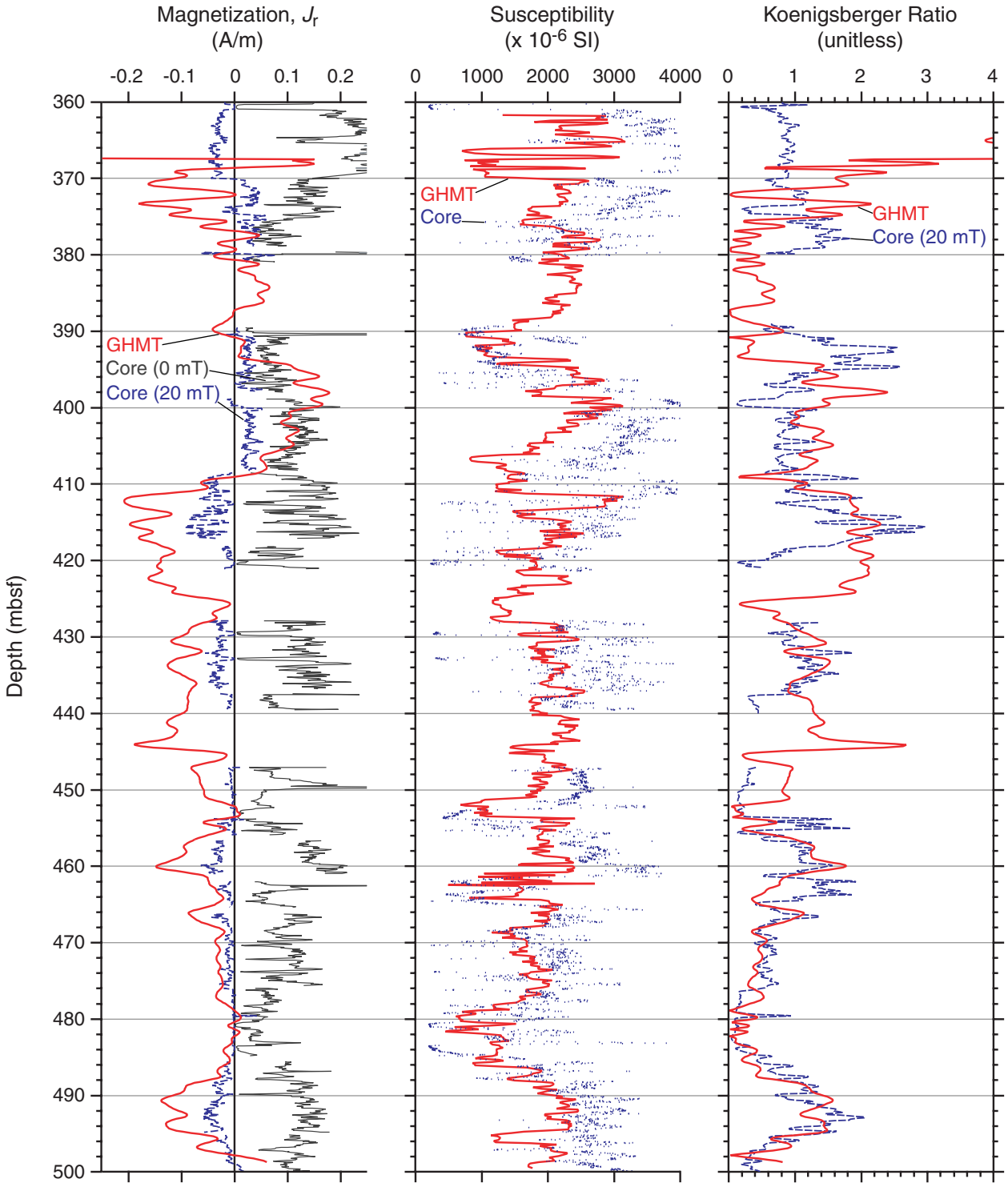

Figure F10. Comparison of time-averaged Koenigsberger ratios in different sediment types (see "Efficiency of Paleomagnetic Recording at Different Sites," p. 8, and Table T2, p. 23).

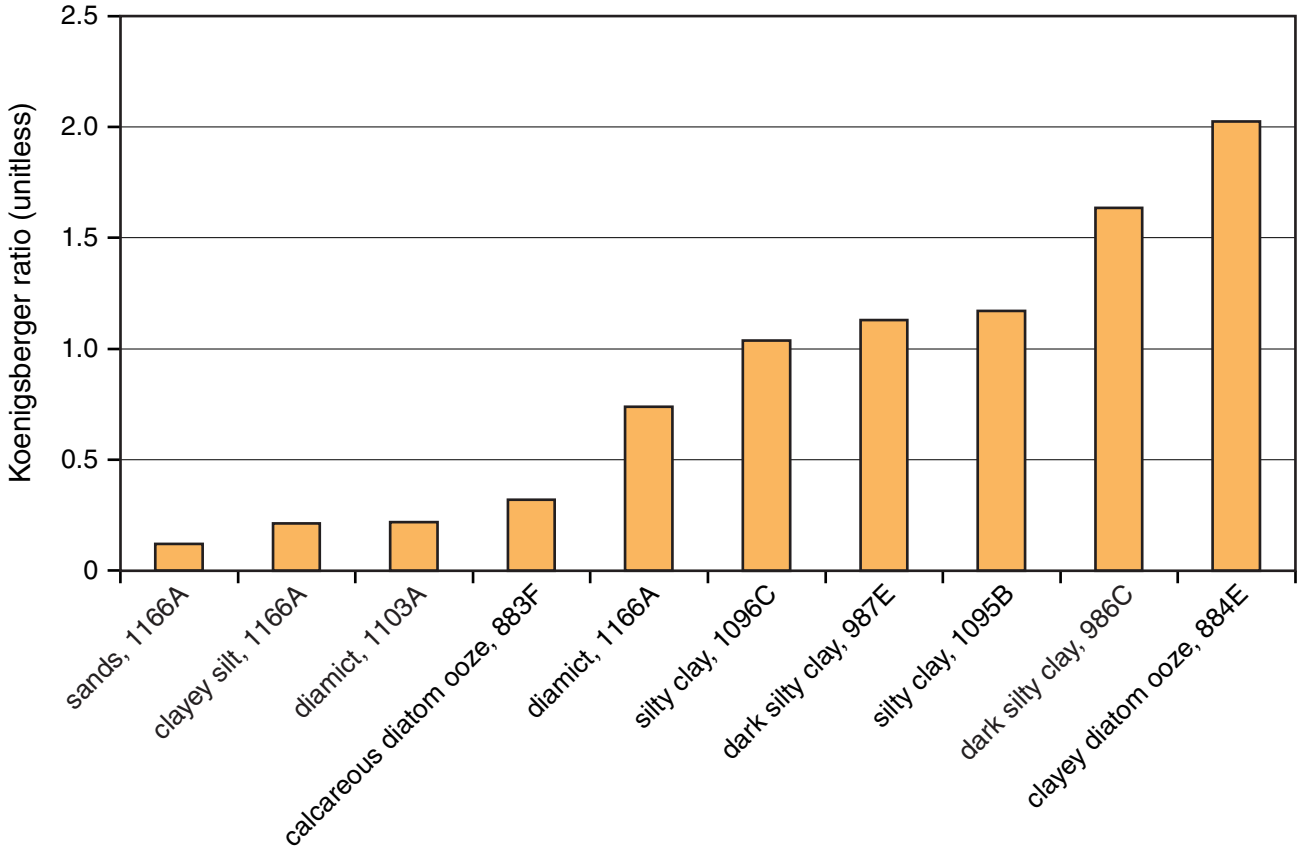

Table T1. IGRF field values for the logged Leg 178 sites.

Hole	Hole depth (mbsf)	Water depth (mbsl)	Latitude	Longitude	Inclination* (°)	B_r* (nT)	$B_r + B_a$† (nT)
1095B	570	3842	66°59′S	78°29′W	–60.46°	44126	~44700
1096C	607	3152	67°34′S	76°57′W	–60.65°	44183	~44250
1103A	362	493	63°59′S	65°27′W	–58.12°	41621	~39000

Notes: IGRF = International Geomagnetic Reference Field. * = IGRF 2000. † = GHMT.

Table T2. Koenigsberger ratios derived from GHMT logs for a selection of ODP sites.

Leg	Hole	Latitude	Interval (mbsf)	Sediment type	Remanent anomaly (nT)	Koenigsberger ratio	Koenigsberger ratio (latitude corrected)
178	1095B	66°59′S	170-530	Silty clay	70 ± 50	1.10	1.17
178	1096C	67°34′S	380-498	Silty clay	60 ± 40	0.96	1.02
178	1103A	64°00′S	214-233	Diamict	30 ± 15	0.20	0.22
188	1166A	67°42′S	60-112	Diamict	70 ± 30	0.30	0.32
188	1166A	67°42′S	165-270	Sands	3 ± 4	0.12	0.13
188	1166A	67°42′S	285-340	Clayey silt	7 ± 8	0.21	0.22
162	986C	77°20′N	145-224	Dark silty clay	60 ± 30	1.59	1.62
162	987E	70°30′N	158-200	Dark silty clay	50 ± 25	1.07	1.12
145	883F	51°12′N	260-700	Calcareous diatom ooze	3 ± 4	0.64	0.76
145	884E	51°27′N	125-410	Clayey diatom ooze	25 ± 14	1.70	2.02

Note: GHMT = geological high-resolution magnetic tool.